

Research Article

Synthesis, Characterization, Biological Activity and Thermal Studies of Trimethoprim Metal Complexes

Mamdouh S. Masoud¹, Alaa E. Ali², Gehan S. Elasal², and Gomaa E. Amer^{2*}

¹Department of Chemistry, Alexandria University, Egypt

²Department of Chemistry, Damanhour University, Egypt

***Corresponding author**

Gomaa E. Amer, Department of Chemistry, Faculty of Science, Damanhour University, Egypt

Submitted: 31 December 2018

Accepted: 24 January 2019

Published: 30 January 2019

ISSN: 2379-089X

Copyright

© 2019 Amer et al.

OPEN ACCESS

Keywords

• Trimethoprim; Complexes; Synthesis; Biological activity; Thermal Studies

Abstract

Nine complexes of trimethoprim with some transition metals [Cr(III), Mn(II), Fe(III), Co(II), Ni(II), Cu(II), Zn(II), Cd(II) and Hg(II)] were synthesized and characterized by elemental analysis, IR, electronic spectra and magnetic measurements. The IR spectra proved that trimethoprim act as a bidentate ligand. From the electronic spectra and magnetic measurements, all complexes have octahedral geometry. The antimicrobial activity examined against two gram-positive and two gram-negative bacteria. The complexes showed a well antifungal activity. The thermal decomposition mechanisms of trimethoprim and its metal complexes were studied and suggested from the DTA and TGA curves. All complexes were thermally decomposed and ended by formation of the metal oxides except the complex of mercury.

INTRODUCTION

Trimethoprim, chemically 5-(3,4,5-trimethoxybenzyl)pyrimidine-2,4-diamine, it is composed of two parts: 3,4,5-trimethoxytoluene and 2,4-diamino-5-methylpyrimidine (Figure 1). It is one of the chemotherapeutic agents known as dihydrofolate reductase inhibitors. It is used in prophylaxis treatment and urinary tract infections [1].

Trimethoprim is a synthetic antibacterial combination product. It is considered as bacteriostatic antibiotic. It acts by interfering with the action of bacterial dihydrofolate reductase, inhibiting synthesis of tetrahydrofolic acid. This is an essential precursor in the de novo synthesis of the intermediate thymidine monophosphate, a precursor of DNA metabolite thymidine triphosphate [2].

Bacteria are unable to take up folic acid from the environment and are thus dependent on their own synthesis. Inhibition of the enzyme deprives the bacteria of nucleotides which are necessary for DNA replication causing, in certain circumstances, cell lethality. Trimethoprim combination with sulphadimidine antibiotic inhibits an earlier step in the folate synthesis pathway (Figure 2). This combination results in an in-vitro synergistic antibacterial effect by inhibiting successive steps in folate synthesis. This benefit was not seen in general clinical use [3]. Trimethoprim has higher antimicrobial activity against gram-positive and gram-negative bacteria and antifungal activity against different fungi. Previous work for trimethoprim metal complexes fell to synthesis of trimethoprim complexes with [Fe, Cu, Zn and Pt] [4]. In this study the coordination properties of trimethoprim metal

complexes were discussed and identified by IR, UV-Vis, ESR and magnetic susceptibility measurements. The thermal behavior of trimethoprim and its metal complexes were discussed from the TGA and DTA curves. The proposed mechanism of decomposition is discussed. Also the thermodynamic and kinetic parameters were calculated. The biological activity of the ligand and its complexes aimed to be studied.

EXPERIMENTAL PART

The solution of trimethoprim was prepared by dissolving the solid in hot ethanol, while the solutions of the salts [Cr(III), Mn(II), Fe(III), Co(II), Ni(II), Cu(II), Zn(II), Cd(II) and Hg(II)] as chlorides were prepared by dissolving the salt in 50 ml distilled water. The solution of trimethoprim was mixed with the aqueous solution of the metal chloride with molar ratio (1:1). The reaction mixture was refluxed for about 45 min then left overnight. The obtained precipitates were isolated by filtration, and then washed by EtOH-H₂O and dried in a vacuum desiccator over anhydrous CaCl₂. The analytical data (Table 1), of the prepared complexes examined by usual methods [5]. The chloride contents of the complexes were analyzed by using Volhard method [6]. Also the contents of metals were determined by using atomic absorption spectroscopy and complexometric analysis [7].

MEASUREMENTS

The electronic spectra of the solid metal complexes were measured in Nujol mull spectra by use Unicam UV/Vis spectrometer [8]. The IR spectra of the trimethoprim and its metal complexes were recorded on Perkin Elmer spectrophotometer, Model

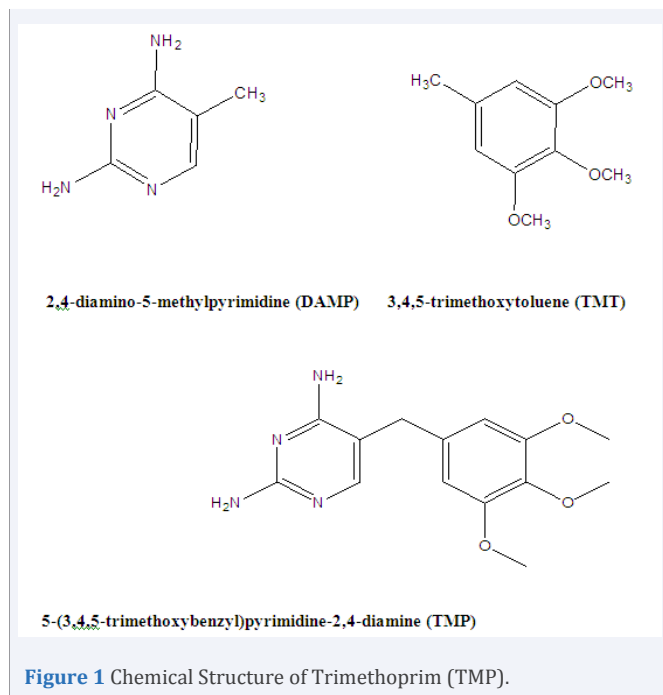


Figure 1 Chemical Structure of Trimethoprim (TMP).

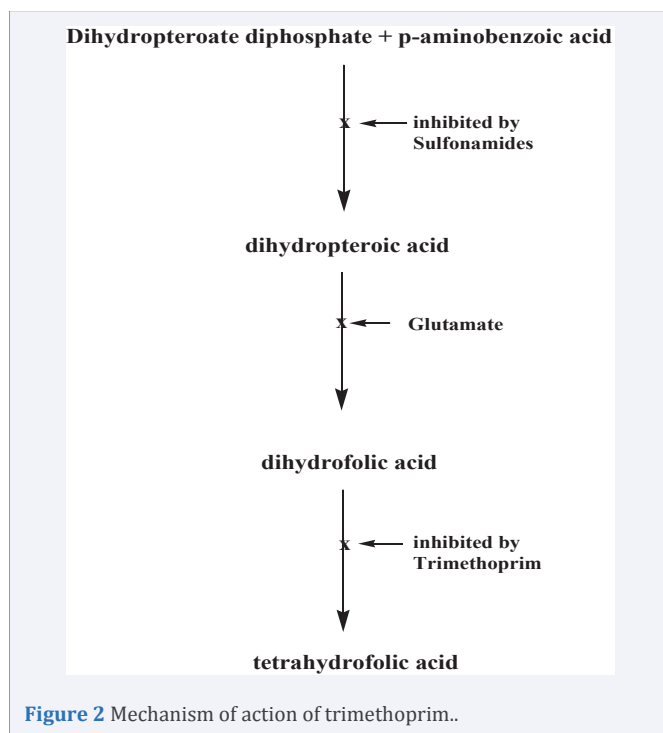


Figure 2 Mechanism of action of trimethoprim..

1430 which it is range of 400-4000 cm^{-1} . The Molar magnetic susceptibilities were determined by using Pascal's constants at room temperature using Faraday's method. The electron spin resonance spectra were recorded on reflection spectrometer operating at (9.1-9.8) GHz in a cylindrical resonance cavity with 100 KHZ modulation. The values of g were determined by comparison with the standard DPPH signal. Differential thermal analysis and thermogravimetric analysis of the ligand and its complexes were recorded on Shimadzu DTA/TGA-60 thermal analyzer with heating rate $10^\circ\text{C}/\text{min}$ under nitrogen atmosphere

of flow rate 20 ml/min. The biological activity of trimethoprim and its complexes were examined against five microorganisms representing different microbial categories, two Gram-positive (Staphylococcus Aureas ATCC6538P and Bacillus subtilis ATCC19659), two Gram negative (*Escherichia coli* ATCC8739 strain and *Pseudomonas aeruginosa* ATCC9027) and candida albicans as a fungi.

RESULTS AND DISCUSSION

The IR of trimethoprim and its metal complexes are listed in (Table 2) with some important characteristic assignments. Trimethoprim showed characteristic bands at 3469, 3317 and 1636 cm^{-1} mainly due to the asymmetric νNH_2 , symmetric νNH_2 and $\nu\text{C}=\text{N}$ pyrimidine ring vibrations, respectively. The metal complexes also contained other bands which are indication of the coordination of the ligand with the metal ions. The asymmetric νNH_2 band appeared at 3469 cm^{-1} in the spectrum of trimethoprim, this band and the $\nu\text{C}=\text{N}$ pyrimidine ring band shifted for trimethoprim metal complexes. Spectral studies of all synthesized trimethoprim metal complexes indicated that the linking of the organic molecule with the metal ions as a bidentate ligand through the nitrogen atom N(7) of the amino group and the nitrogen atom N(2) of the pyrimidine ring. For $[\text{Cr}(\text{TMP})\text{Cl}_2(\text{OH})\text{H}_2\text{O}]\cdot\text{H}_2\text{O}$ complex, the coordination occurred through the nitrogen atom of amino group which was indicated by shifting of νNH_2 from 3469 cm^{-1} to 3406 cm^{-1} and the nitrogen atom of pyrimidine ring which was indicated by shifting of $\nu\text{C}=\text{N}$ from 1636 to 1675 cm^{-1} , Table 2, besides appearance of $\nu\text{M}-\text{N}$ stretching at 507 cm^{-1} , $\nu\text{M}-\text{O}$ stretching at 490 cm^{-1} [9], and $\nu\text{M}-\text{Cl}$ at 450 cm^{-1} , Table 2. For the complex $[\text{Mn}(\text{TMP})_2\text{Cl}_2]\cdot\text{H}_2\text{O}$, the shift in the amino group from 3469 to 3405 cm^{-1} and the change in the value of $\nu\text{C}=\text{N}$ of from 1636 to 1674 cm^{-1} , Table 2, indicated that the coordination occurred through the nitrogen atoms of amino group and of pyrimidine ring, so the ligand acts as bidentate, in addition to appearance of bands at 518 cm^{-1} and 465 cm^{-1} , Table 2, represents $\nu\text{M}-\text{N}$ stretching and $\nu\text{M}-\text{Cl}$ respectively. Similar situations are evident for all the other complexes Table 2. The electronic absorption spectra for the chromium complex $[\text{Cr}(\text{TMP})\text{Cl}_2\text{OHH}_2\text{O}]\cdot\text{H}_2\text{O}$ showed three bands at 295, 405, 600 nm due to $4\text{A}_2\text{g}\rightarrow 4\text{T}_1\text{g}(\text{P})$, $4\text{A}_2\text{g}\rightarrow 4\text{T}_1\text{g}(\text{F})$ and $4\text{A}_2\text{g}\rightarrow 4\text{T}_2\text{g}(\text{F})$ transitions, respectively (Table 3). So the complex has octahedral geometry. Such octahedral geometry is deduced from the μ_{eff} value which equals, 4.71 B.M [10,11]. However, the electronic absorption spectra of the buff manganese complex, $[\text{Mn}(\text{TMP})_2\text{Cl}_2]\cdot\text{H}_2\text{O}$, (Table 3), gave bands at 310, 353 and 500 nm where the first band is assigned to $6\text{A}_1\text{g}\rightarrow 4\text{A}_1\text{g}$ transition, while the second band is due to $6\text{A}_1\text{g}\rightarrow 4\text{T}_2\text{g}$ transition and the last band is due to $6\text{A}_1\text{g}\rightarrow 4\text{T}_1\text{g}$ transition [12,13]. Its room temperature μ_{eff} value of 4.30 B.M, typified the existence of Oh geometry. The electronic absorption spectra of pale brown iron complex, $[\text{Fe}(\text{TMP})\text{Cl}_2(\text{OH})\text{H}_2\text{O}]\cdot 2\text{H}_2\text{O}$, (Table 3), gave bands at 258, 350, 483 nm . These bands are due to CT ($\text{t}_2\text{g}\rightarrow \pi^*$) and CT ($\pi\rightarrow \text{eg}$). Its room temperature μ_{eff} value of 4.26 B.M, typified the existence of Oh configuration [14,15]. The spectra for the pale pink $[\text{Co}(\text{TMP})_2\text{Cl}_2]\cdot 3\text{H}_2\text{O}$ complex, (Table 3), gave bands at 294, 473, 558 nm . The bands are due to charge transfer, while the latter broad band is assigned to $4\text{T}_1\text{g}(\text{F})\rightarrow 4\text{T}_1\text{g}(\text{P})$ transition with $\mu_{\text{eff}} = 5.13\text{ B.M}$, typified the existence of octahedral geometry [16]. The green electronic absorption spectra for the $[\text{Ni}(\text{TMP})_2\text{Cl}_2]\cdot\text{H}_2\text{O}$ complex showed three bands at 381, 480

Table 1: Elemental analysis, m.p. and color of trimethoprim metal complexes.

| Complexes | Color | Calculated/(Found)% | | | | |
|---|-------------|---------------------|----------------|------------------|------------------|------------------|
| | | C | H | N | M | Cl |
| [Cr(TMP)Cl ₂ (OH)H ₂ O].H ₂ O | Pale blue | 36.06 (36.11) | 4.97 (4.93) | 12.02 (12.11) | 11.15 (11.21) | 15.21 (15.18) |
| [Mn(TMP) ₂ Cl ₂].H ₂ O | Buff | 46.42 (46.47) | 5.29 (5.32) | 15.47 (15.41) | 7.58 (7.49) | 9.79 (9.63) |
| [Fe(TMP)Cl ₂ (OH)H ₂ O].2H ₂ O | Pale brown | 34.45 (34.48) | 5.16 (5.12) | 11.48 (11.43) | 11.44 (11.46) | 14.53 (14.54) |
| [Co(TMP) ₂ Cl ₂].3H ₂ O | Pale pink | 43.99 (44.03) | 5.54 (5.49) | 14.66 (14.59) | 7.71 (7.76) | 9.27 (9.22) |
| [Ni(TMP) ₂ Cl ₂].H ₂ O | Green | 46.18 (46.21) | 5.26 (5.28) | 15.39 (15.36) | 8.06 (8.12) | 9.74 (9.81) |
| [Cu(TMP) ₂ Cl ₂].H ₂ O | Pale green | 45.87 (45.91) | 5.22 (5.19) | 15.28 (15.25) | 8.67 (8.58) | 9.67 (9.63) |
| [Zn(TMP) ₂ Cl ₂].H ₂ O | Colorless | 45.76 (45.71) | 5.21 (5.26) | 15.25 (15.19) | 8.90 (8.98) | 9.65 (9.59) |
| [Cd(TMP) ₂ Cl ₂].H ₂ O | Pale yellow | 43.01 (43.06) | 4.90 (4.88) | 14.33 (14.28) | 14.38 (14.40) | 9.07 (9.13) |
| [Hg(TMP) ₂ Cl ₂].H ₂ O | White | 38.65 (38.58) | 4.40 (4.42) | 12.88 (12.90) | 23.05 (22.96) | 8.15 (8.08) |

The melting point of the all prepared complexes is higher than 300^o C

Table 2: Fundamental infrared bands of trimethoprim (cm⁻¹) and its metal complexes.

| Compounds | ν_{NH_2} | $\nu_{\text{C=N}}$ | $\nu_{\text{M-N}}$ | $\nu_{\text{M-O}}$ | $\nu_{\text{M-Cl}}$ |
|---|---------------------|--------------------|--------------------|--------------------|---------------------|
| TMP | 3469 | 1636 | | | |
| [Cr(TMP)Cl ₂ (OH)H ₂ O].H ₂ O | 3406 | 1675 | 507 | 470 | 430 |
| [Mn(TMP) ₂ Cl ₂].H ₂ O | 3405 | 1674 | 518 | | 438 |
| [Fe(TMP)Cl ₂ (OH)H ₂ O].2H ₂ O | 3402 | 1670 | 519 | 466 | 435 |
| [Co(TMP) ₂ Cl ₂].3H ₂ O | 3405 | 1675 | 507 | | 420 |
| [Ni(TMP) ₂ Cl ₂].H ₂ O | 3405 | 1674 | 517 | | 425 |
| [Cu(TMP) ₂ Cl ₂].H ₂ O | 3405 | 1674 | 518 | | 431 |
| [Zn(TMP) ₂ Cl ₂].H ₂ O | 3428 | 1673 | 528 | | 438 |
| [Cd(TMP) ₂ Cl ₂].H ₂ O | 3415 | 1670 | 577 | | 435 |
| [Hg(TMP) ₂ Cl ₂].H ₂ O | 3408 | 1623 | 575 | | 430 |

Electronic spectra and magnetic studies**Table 3:** Nujol mull electronic absorption spectra λ_{max} (nm), room temperature effective magnetic moment values (μ_{eff} , 298^oK) and geometries of trimethoprim metal complexes.

| Complex | λ_{max} (nm) | μ_{eff} (B.M) | Geometry |
|---|-----------------------------|--------------------------|----------------|
| [Cr(TMP)Cl ₂ (OH)H ₂ O].H ₂ O | 295, 405, 600 | 4.71 | O _h |
| [Mn(TMP) ₂ Cl ₂].H ₂ O | 310, 353, 500 | 4.30 | O _h |
| [Fe(TMP)Cl ₂ (OH)H ₂ O].2H ₂ O | 258, 350, 483 | 4.26 | O _h |
| [Co(TMP) ₂ Cl ₂].3H ₂ O | 294, 473, 558 | 5.13 | O _h |
| [Ni(TMP) ₂ Cl ₂].H ₂ O | 381, 480, 625 | 2.80 | O _h |
| [Cu(TMP) ₂ Cl ₂].H ₂ O | 260, 410, 720 | 2.09 | O _h |
| [Zn(TMP) ₂ Cl ₂].H ₂ O | | Diamagnetic | O _h |
| [Cd(TMP) ₂ Cl ₂].H ₂ O | | Diamagnetic | O _h |
| [Hg(TMP) ₂ Cl ₂].H ₂ O | | Diamagnetic | O _h |

and 625 nm due to 3A₂g(F)→3T₁g(P) and 3A₂g(F)→3T₁g(F) transitions, respectively, (Table 3) with octahedral geometry, further deduced from the μ_{eff} value which equal 2.80 B.M. The pale green copper complex [Cu(TMP)₂Cl₂].H₂O, (Table 3), exhibited bands at 260, 410 and 720 nm assigned to 2E_g → 2T_{2g} transition suggesting octahedral geometry (Figure 3) [17], with room temperature μ_{eff} value 2.09 B.M. The complexes of zinc, cadmium and mercury are diamagnetic with d¹⁰ configuration,

so no d-d transition could be observed. The geometry of zinc, cadmium and mercury complexes was octahedral depending on elemental analysis.

Electron spin resonance of copper complex

The room temperature solid state ESR spectrum of [Cu(TMP)₂Cl₂].H₂O complex (1:2), Figure 4 exhibit an isotropic nature where $g_s = 2.173$ with value of $A = 148$ ($\times 10^{-4}$ cm⁻¹).

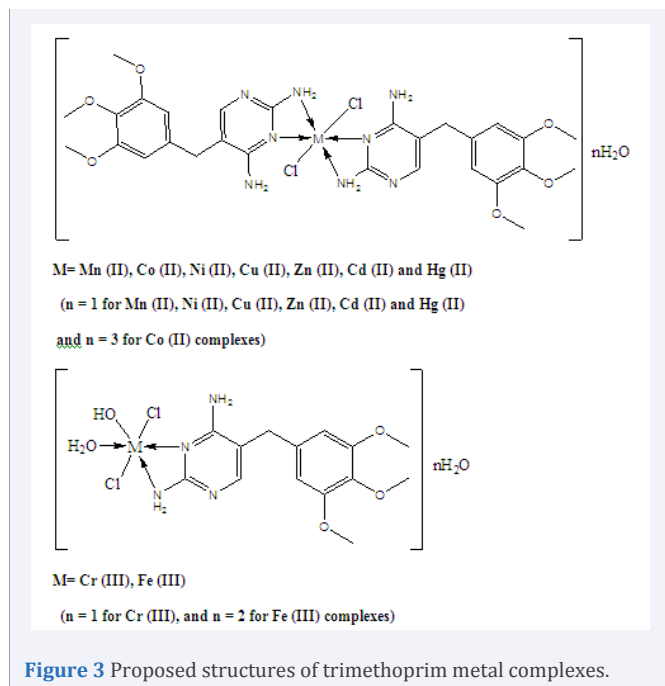


Figure 3 Proposed structures of trimethoprim metal complexes.

Biological activity

The antimicrobial activities of the synthesized complexes have been screened *in vitro*, as growth inhibiting agents. The antibacterial and antifungal screening were carried out using disc diffusion method [18] against some strains of bacteria like *Staphylococcus aureus* (ATCC 6538P), *Bacillus subtilis* (ATCC 19659); (Gram positive), *Escherichia coli* (ATCC 8739) and *Pseudomonas aeruginosa* (ATCC 9027); (Gram negative) and one fungal species *Candida albicans* (ATCC 2091). The compounds were dissolved in DMSO (1mg/ml). The study included trimethoprim and four complexes of different metal ions (cobalt, nickel, copper and zinc). Two different broadly antibiotics (Ciprofloxacin and Clotrimazole) are used in this study as references. After incubation for 24 h at 37°C in the case of bacteria and for 48 h at 37°C in the case of fungi, inhibition of the organisms was evidenced by clear zone surrounding each disk, measured in millimeters [19]. Trimethoprim and its all complexes showed high antimicrobial activity. The ligand showed inhibition zone 33 for Gram-positive bacteria (*Staphylococcus aureus*) and inhibition zone 30 for Gram negative bacteria (*Escherichia coli*) (Table 4). Also, it showed antifungal effect with inhibition zone 25. The $[Co(TMP)_2Cl_2] \cdot 3H_2O$ complex showed activity for *Staphylococcus aureus* and *Escherichia coli* with inhibition zones 29 and 27, respectively. The complex has also activity against *Candida albicans* with inhibition zone 17. The complexes $[Ni(TMP)_2Cl_2] \cdot H_2O$, and $[Zn(TMP)_2Cl_2] \cdot H_2O$ showed activity for *Staphylococcus aureus* with inhibition zones 30. While for *Escherichia coli* the inhibition zones were 27. The $[Cu(TMP)_2Cl_2] \cdot H_2O$ complex showed activity against *Staphylococcus aureus* and *Escherichia coli* with inhibition zones 30 and 24, respectively. Trimethoprim and its metal complexes showed no activity against *Pseudomonas aeruginosa* and *Bacillus subtilis*, while they appeared a well antifungal activity with *Candida albicans* (Table 4).

Thermal analysis

The thermal analysis of some coordination compounds has been reported from Masoud et al [20-24]. The study of thermal analysis of the ligand (trimethoprim) and its metal complexes were investigated. In this study different techniques were used: thermogravimetric analysis (TGA) and differential thermal analysis (DTA). The data of analysis are collected in Table 5. In case of the free ligand (trimethoprim), the decomposition occurred in three steps in temperature range 36.6-597.4°C, Figure 5. The first step of decomposition at 36.6°C, the weight loss was 9.21%. The step ended at 255.5°C. The second step of decomposition started above 256°C and the weight loss was 42.02%, this step ended at 401.7°C. While the last step was in temperature range between 402-600°C, and the weight loss was 48.66%. All steps accompanied by the endothermic effect in the DTA curve in the range of temperature from 19.7 to 600°C. All TGA steps were ended by no residue. The suggested mechanism of decomposition is given in Figure 6.

For the $[Cr(TMP)Cl_2(OH)H_2O] \cdot H_2O$ complex, Figure 7, the decomposition occurred in three steps. The first step of decomposition above 30°C, the weight loss was 12.91% and ended at 232.0°C which accompanied by the endothermic effect in the DTA curve at temperature 200°C. The second step of decomposition started above 240 °C and the weight loss was 33.52%, this step ended at 375°C. While the last step was in temperature range between 380-505.4°C, and the weight loss was 37.33%. The second and the last steps in TGA are overlapped to give an exothermic peak in DTA thermogram which appeared in temperature range 240-600°C. The first endothermic peak is due to dehydration of water molecules and loss of ethylene. The rest strong peaks are due to decomposition steps of the complex ended with the formation of 0.5 Cr₂O₃ as a final product. The suggested mechanism of decomposition is given in Figure 8.

Meanwhile, the $[Hg(TMP)_2Cl_2] \cdot H_2O$ complex, Figure 9, decomposed in three steps, there is no mass change to 35.9°C.

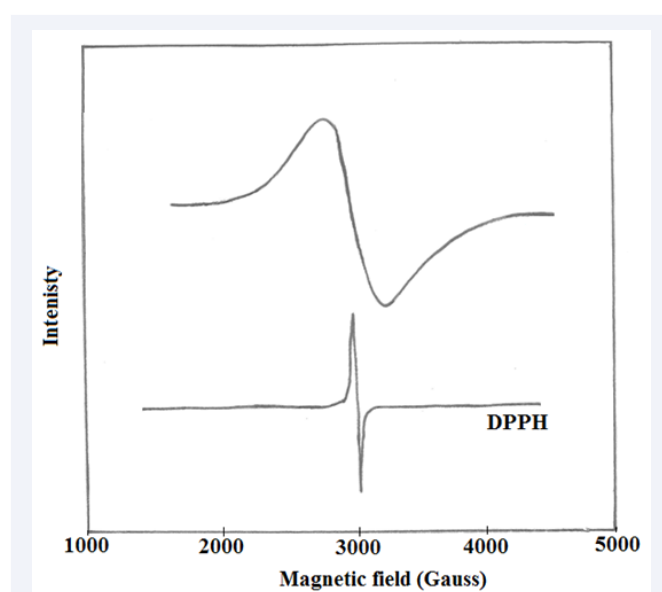


Figure 4 X-band ESR spectra of $[Cu(TMP)_2Cl_2] \cdot H_2O$ complex.

Table 4: Antibacterial and antifungal activity of the investigated compounds against some reference strains expressed in absolute activity (AU).

| Compound | Blank | <i>Staphylococcus aureus</i> | <i>Bacillus subtilis</i> | <i>Pseudomonas aeruginosa</i> | <i>Escherichia coli</i> | <i>Candida albicans</i> |
|---|-------|------------------------------|--------------------------|-------------------------------|-------------------------|-------------------------|
| Trimethoprim | 8 | 33 | 8 | 8 | 30 | 25 |
| [Co(TMP) ₂ Cl ₂].3H ₂ O | 8 | 29 | 8 | 8 | 27 | 17 |
| [Ni(TMP) ₂ Cl ₂].H ₂ O | 8 | 30 | 8 | 8 | 27 | 20 |
| [Cu(TMP) ₂ Cl ₂].H ₂ O | 8 | 30 | 8 | 8 | 24 | 20 |
| [Zn(TMP) ₂ Cl ₂].H ₂ O | 8 | 30 | 8 | 8 | 27 | 19 |
| Ciprofloxacin | 9 | 30 | 30 | 30 | 30 | - |
| Clotrimazole | 10 | - | - | - | - | 17 |

Table 5: DTA analysis of trimethoprim and its metal complexes.

| Compound | Type | T _m (°K) | E _a (kJ mol ⁻¹) | n | α _m | ΔS [#] (kJ K ⁻¹ mol ⁻¹) | ΔH [#] (kJ mol ⁻¹) | Z (S ⁻¹) | Temp. (°C) TGA | Wt. Loss % | | Assignment |
|---|------|---------------------|--|------|----------------|---|---|----------------------|----------------------------|----------------|----------------|---|
| | | | | | | | | | | Calc | Found | |
| Trimethoprim | Endo | 487 | 6.38 | 1.19 | 0.60 | -0.322 | -156.71 | 0.002 | 36.6-255.5 255.5-401.7 | 9.64 42.02 | 9.21 42.01 | Elimination of CH ₂ CH ₂ . Loss of CO ₂ and C ₆ H ₆ . |
| | Endo | 723 | 20.77 | 1.27 | 0.59 | -0.319 | -230.311 | 0.003 | 401.7-597.4 | 48.23 | 48.66 | Elimination of the rest of ligand forming no residue. |
| [Cr(TMP)Cl ₂ (OH)H ₂ O].H ₂ O | Endo | 345 | 9.27 | 1.26 | 0.59 | -0.313 | -107.97 | 0.003 | 20.9-232.0 | 13.72 | 12.91 | Loss of 2H ₂ O and CH ₂ CH ₂ . |
| | Exo | 759 | 43.24 | 1.34 | 0.58 | -0.313 | -237.764 | 0.007 | 232.0-375.0 375.0-505.4 | 33.97 35.92 | 33.52 37.33 | Loss of CO ₂ , C ₆ H ₆ and HCl. Elimination of the rest of ligand and forming 0.5Cr ₂ O ₃ . |
| [Mn(TMP) ₂ Cl ₂].H ₂ O | Endo | 366 | 22.07 | 1.52 | 0.55 | -0.307 | -112.26 | 0.007 | 32.1-237.8 | 55.32 | 55.88 | Loss of H ₂ O, 2HCl, 2C ₆ H ₆ , C ₂ H ₂ , 3CO and CH ₃ COH. |
| | Exo | 771 | 36.66 | 1.17 | 0.60 | -0.315 | -242.782 | 0.006 | 237.8-418.7 418.7-598.1 | 4.13 20.70 | 3.54 20.17 | Elimination of N ₂ H ₂ . Elimination of the rest of ligand, forming MnO+6C. |
| [Fe(TMP)Cl ₂ (OH)H ₂ O].2H ₂ O | Endo | 358.4 | 10.01 | 2.18 | 0.48 | -0.313 | -112.162 | 0.003 | 35.8-201.2 | 11.06 | 10.99 | Elimination of 3H ₂ O. |
| | Exo | 585 | 119.36 | 1.28 | 0.59 | -0.300 | -175.786 | 0.025 | 201.2-415.8 | 34.91 | 34.74 | Elimination of 3C ₂ H ₂ , HCl and 2CO. |
| | Exo | 801 | 33.01 | 1.02 | 0.63 | -0.316 | -253.436 | 0.005 | 415.8-565.1 | 37.57 | 38.07 | Elimination of the rest of ligand, forming 0.5Fe ₂ O ₃ . |
| [Co(TMP) ₂ Cl ₂].3H ₂ O | Endo | 457 | 7.51 | 1.19 | 0.59 | -0.319 | -145.956 | 0.002 | 36.0-163.7 163.7-279.6 | 7.07 7.85 | 7.97 8.27 | Elimination of 3H ₂ O. Elimination of 2H ₂ CO. |
| | Exo | 613 | 105.27 | 1.33 | 0.58 | -0.302 | -185.316 | 0.021 | 279.6-443.5 | 36.48 | 35.05 | Elimination of Cl ₂ , 2CO and 2C ₆ H ₆ . |
| | Exo | 753.4 | 145.29 | 1.41 | 0.57 | -0.303 | -228.326 | 0.023 | 443.5-556.0 | 38.45 | 38.85 | Elimination of the rest of ligand, forming CoO. |

the first step started at 36°C, the weight loss was 56.51% and ended at 157.2°C, this step accompanied by the endothermic effect in the DTA curve at temperature 89°C. The second step of decomposition started above 158°C and the weight loss was 15.45%. The step ended at 265.9°C. The last step decomposed above 266°C, and the weight loss was 25.09% and ended at 595.9°C. The second and last steps accompanied by the exothermic effect in the DTA curve at temperature 332°C. All TGA steps are due to dehydration process of water molecule, sublimation of Hg in temperature range 266-595.9°C and decomposition steps

of the complex ended by formation of carbon residue as a final product with 2.8%. The suggested mechanism of decomposition is given in Figure 10.

CONCLUSION

The complexes of trimethoprim was synthesized and characterized by different spectroscopic methods. The stoichiometry of complexes was determined by the analytical data. All complexes have octahedral geometries. The Nujol mull electronic spectra confirmed these results. An ESR spectrum of

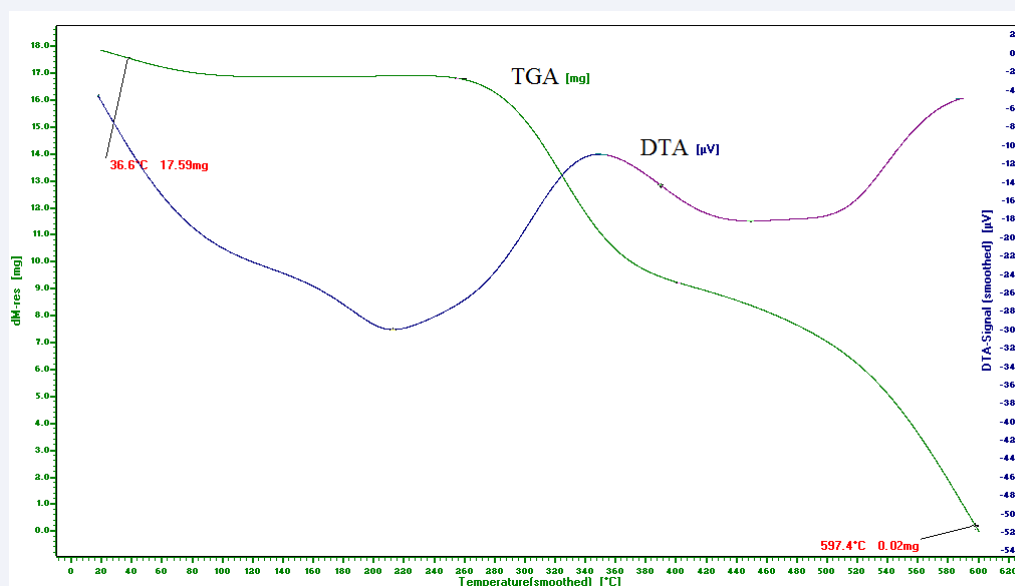


Figure 5 TGA and DTA curves for trimethoprim.

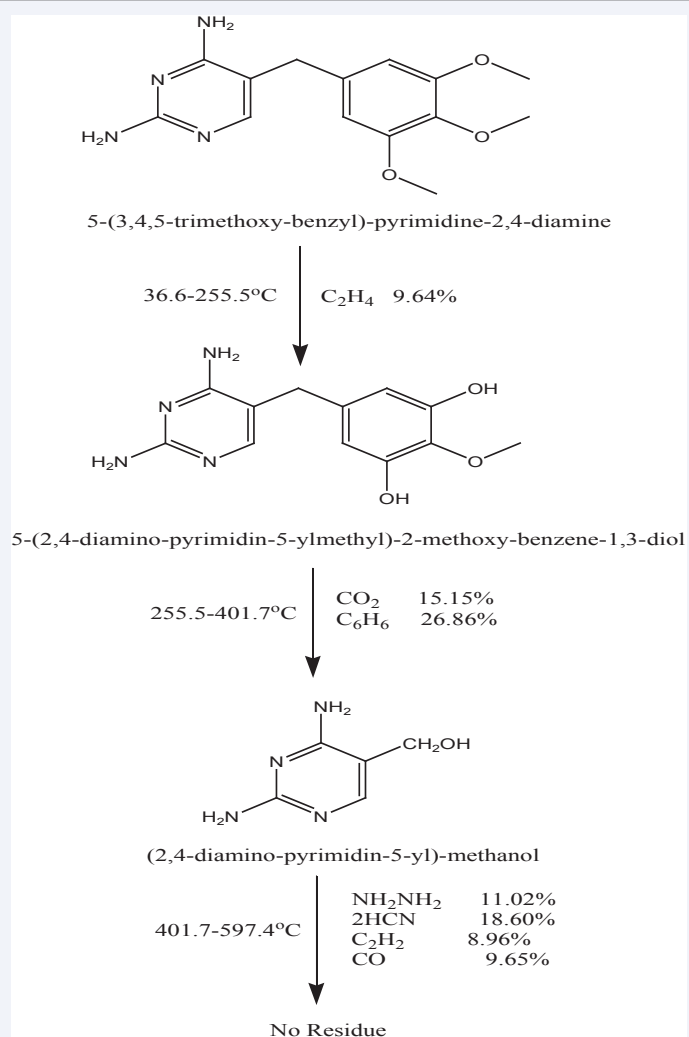


Figure 6 Thermolysis of Trimethoprim.

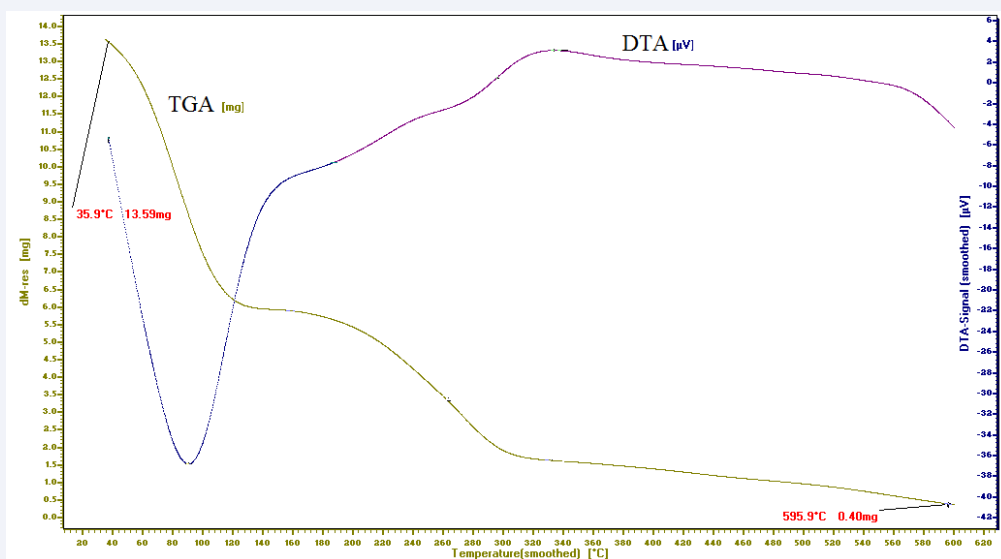


Figure 9 TGA and DTA curves for $[Hg(TMP)_2Cl_2].H_2O$ complex.

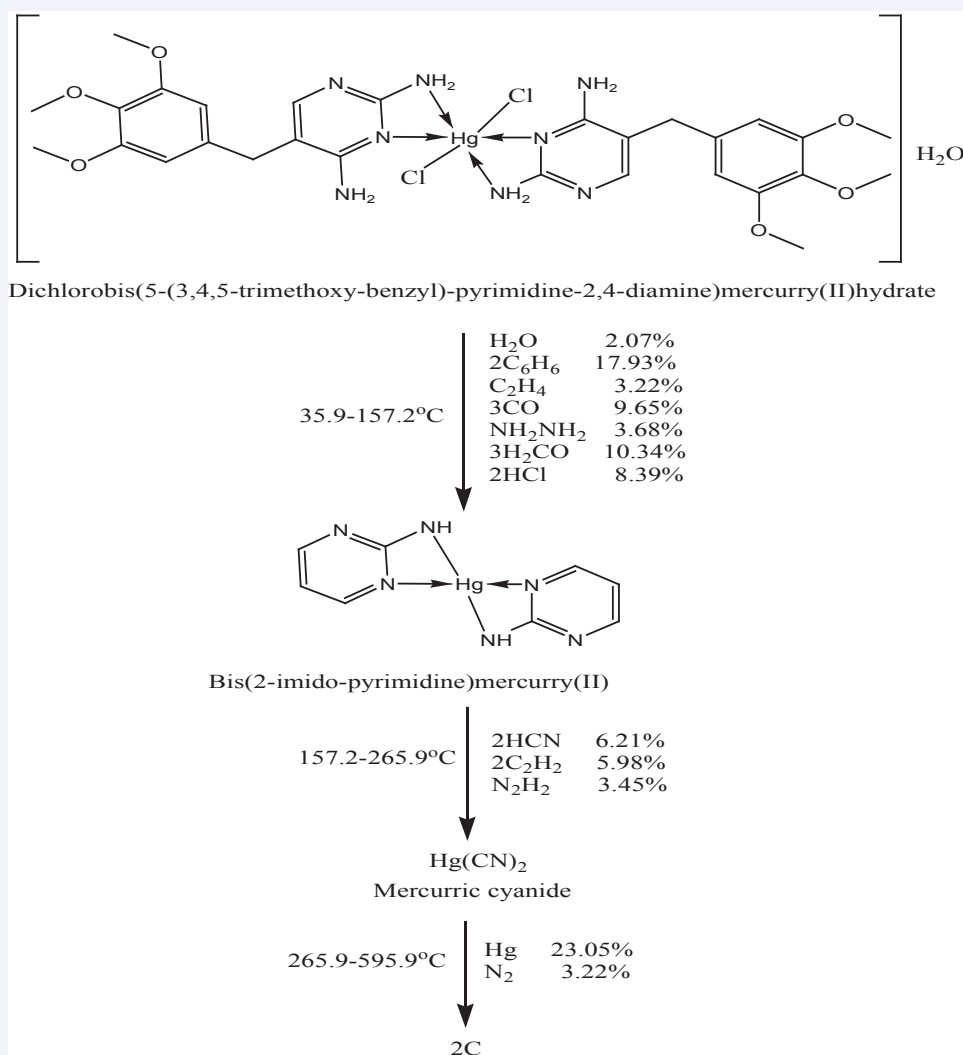


Figure 10 Thermolysis of $[Hg(TMP)_2Cl_2].H_2O$ complex.

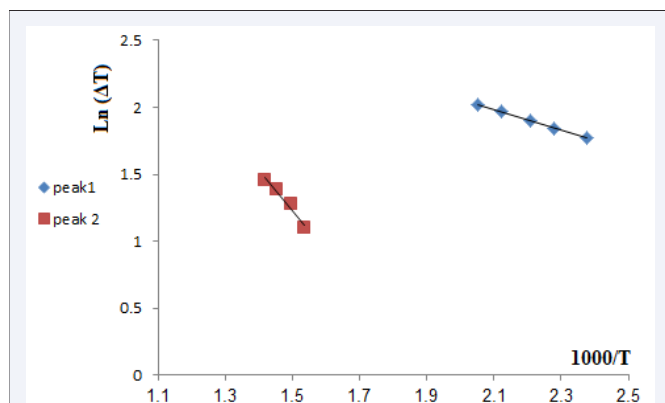


Figure 11 Determination of E_a by the relation of $\ln\Delta T$ against $10^3/T$ for trimethoprim ligand.

copper complex was studied. The spectral data confirmed that trimethoprim acts as a bidentate ligand. Trimethoprim showed higher antibacterial and antimicrobial activity than the prepared complexes for some strains. The kinetic and thermodynamic parameters were calculated from the differential thermal analysis curves. All complexes were thermally decomposed and ended by formation of metal oxides except the complex of mercury.

REFERENCES

- Rajith L, Kumar KG. The role of banned substance residue analysis in the control of dietary supplement contamination. *Drug Testing and Analysis*. 2010; 2: 436-441.
- Brumfitt W, Hamilton-Miller JMT. Reassessment of the Rationale for the Combinations of Sulfonamides with Diaminopyrimidines. *J Chemotherapy*. 1993; 5: 465-469.
- Lawrenson RA, Logie JW. Antibiotic failure in the treatment of urinary tract infections in young women. *J Antimicrobial Chemotherapy*. 2001; 48: 895-901.
- Demirezen N, Tarınc D, Polat D, Çeşme M, Gölcü A, Tümer M. Synthesis of trimethoprim metal complexes: Spectral, electrochemical, thermal, DNA-binding and surface morphology studies. *Spectrochim Acta A*. 2012; 94: 243-255.
- Vogel AI. *A Text Book of Quantitative Inorganic Analysis*, Longmans, London. 1989.
- Lee RH, Griswold E, Kleinberg. Studies on the Stepwise Controlled Decomposition of 2,2'-Bipyridine Complexes of Cobalt(II) and Nickel(II) Chlorides. *J Inorg Chem*. 1964; 3: 1278-1283.
- Schwarzenbach G. *Complexometric Titration*, Translated by H, Methuen Co., London, Irving. 1957.
- El-Asmy AA, Al-Hazmi GAA. Synthesis and spectral feature of benzophenone-substituted thiosemicarbazones and their Ni(II) and Cu(II) complexes. *Spectrochimica Acta A*. 2009; 71: 1885-1890.
- Price ER, Wasson JR. Ligating, Spectral and Thermal Properties of Febuxostat Metal Complexes. *J Inorg Nucl Chem*. 1974; 36: 711-716.
- Howlader MBH, Islam MS, Karim MR. Synthesis of some 16-membered macrocyclic complexes of chromium (III), manganese (II), iron(III), cobalt (II), nickel (II) and copper (II) containing a tetraoxooctaazacyclohexadecane ligand. *J Chem*. 2000; 39: 407-409.
- Sreekanth A, Joseph M, Fun HK, Kurup MRP. Formation of manganese (II) complexes of substituted thiosemicarbazones derived from 2-benzoylpyridine: Structural and spectroscopic studies. *Polyhedron*. 2006; 25: 1408-1414.
- Buhl F, Sroka BS. Desorption/Ionization on Silicon Time-of-Flight/Time-of-Flight Mass Spectrometry. *Chem Anal*. 2003; 48: 58-145.
- Thakar A, Joshi K, Pandya K, Pancholi A. Crystal structure of 2-(3-chloro-phenyl)-5-methyl-4-[1-(5-methyl-4-ptolyl-thiazol-2-ylimino)-ethyl]-2,4-dihydro-pyrazol-3-one, C₂₃H₂₁ClN₄O₅. *J Chem*. 2011; 8: 1750-1764.
- Sokolov VI, Pustovarov VA, Churmanov VN, Ivanov VY, Gruzdev NB, Sokolov. Unusual x-ray excited luminescence spectra of NiO suggest self-trapping of the d-d charge-transfer exciton. *JETP letters*. 2012; 95: 528-533.
- Lever ABP. *Inorganic electronic spectroscopy*. Elsevier publish Co, Amsterdam. 1968; 420.
- Barefield EK, Busch DH, Nelson SM. The Effects of Metal Ion and Ligand Substitution on the Spectroscopic Properties of Metal Complexes. *Quart Rev*. 1968; 22: 457- 498.
- Lokhande MV, Choudhary MR. Some transitional metal ions Complexes With 3-[[([E)-(4-fluorophenyl) methylidene] amino} benzoic acid and its Microbial Activity. *Int J Pharm Sci Res*. 2014; 5: 1757.
- Balouiri M, Sadiki M, Ibsouda SK. Methods for *in vitro* evaluating antimicrobial activity: A review: A Review. *J Pharm Ana*. 2016; 6: 71-79.
- Gull P, Hashmi AA. Biological Activity Studies on Metal Complexes of Macrocyclic Schiff Base Ligand: Synthesis and Spectroscopic Characterization. *J Braz Chem Soc*. 2017; 26: 1331-1337.
- Masoud MS, Ali AE, Ahmed HM, Mohamed EA. Spectral studies and thermal analysis of new vanadium complexes of ethanolamine and related compounds. *J Mol Str*. 2013; 1050: 43-52.
- Masoud MS, Ali AE, Elsalas GS. Spectroscopic behavior and equilibrium studies of some metallocephalosporins. *Spectrochim Acta A*. 2015; 149: 363-377.
- Masoud MS, Ali AE, Ghareeb DA, Nasr NM. Synthesis, characterization, spectral, thermal analysis and computational studies of thiamine complexes. *J Mol Str*. 2015; 1099: 359-372.
- Masoud MS, Ali AE, Elsalas GS, Kolkaila AS. *J chem Pharm Res. Spectroscopic Studies and Thermal Analysis on Cefoperazone Metal Complexes*. 2017; 9: 171-179.
- Masoud M.S, Ali AE, Elsalas GS, Kolkaila AS. Synthesis, spectroscopic, biological activity and thermal characterization of ceftazidime with transition metals. *Spectrochim Acta A*. 2018; 193: 458-466.

Cite this article

Masoud MS, Ali AE, Elsalas GS, Amer GE (2019) Synthesis, Characterization, Biological Activity and Thermal Studies of Trimethoprim Metal Complexes. *J Drug Des Res* 6(1): 1074.